International Journal of Science and Research (IJSR)
ISSN: 2319-7064
Impact Factor 2024: 7.101

Annealing- Induced Changes in the Optical Properties of Hydrogenated Amorphous Silicon Thin Films Fabricated by High-Power PECVD

Aravind Kumar[1], Pawan Kumar[2], Chanchal Kaushik[3], Sai Tripti Samal[4], Monika Bassi[5], Rashmi Menon[6]

[1]Department of Physics Kalindi College University of Delhi-110008
Corresponding Author Email: *arvindkumar[at]kalindi.du.ac.in*

[2]Department of Physics Gurukula Kangri Vishwavidyalaya, Haridwar-249404

[3, 4, 5, 6]Department of Physics Kalindi College University of Delhi-110008

Abstract: ***The crystallization of hydrogenated amorphous silicon (a-Si:H) thin films was deposited by plasma-enhanced chemical vapor deposition technique (PECVD), shows significant scientific and technological interest. Conventionally, crystallization in a-Si:H films is achieved, through thermal annealing or metal-induced crystallization. Our study focus that (a-Si:H) thin films deposited at high radio frequency (RF) power (>0.2 W/cm²) using the PECVD technique (HR-031 at 1 W and Sample no HR-022 at 7 W),ie exhibit embedded crystallites within the (a-Si:H) matrix. Furthermore, post-deposition vacuum thermal annealing at 250°C and 300°C expedites an increase in crystallite size. UV-Vis spectroscopy were analyzed the optical properties and records the absorption or Transmission spectra. Electrical conductivity, dark conductivity and photo conductivity of (a-Si:H) thin films were measured as a function of temperature within the range of 300°C to 250°C. The structural properties were measured using Raman Spectra, FT-IR, XRD (X – Ray diffraction), SEM and Atomic Force Microscopy (AFM). The conductivity values were evaluated both before and after the annealing process. Atomic force microscopy (AFM) analysis confirmed the presence of crystallites in the annealed films, providing insight into the surface morphology and structural modifications induced by thermal annealing.***

Keywords: PECVD Technique**,** crystallization, annealing, conductivity, Transmission spectra

1. Introduction

Plasma-Enhanced Chemical Vapor Deposition (PECVD) of silane has emerged as a advanced and widely adopted technique for the deposition of (a-Si:H) thin films and its related alloys. (a-Si:H) films [1, 2] have attracted significant interest due to their superior optical properties [3,4] and are extensively utilized in photovoltaic applications and large-area electronic devices at the commercial scale. However, the primary challenges associated with this material include its low deposition rate and stability. Therefore, enhancing the deposition rate while preserving the device-grade quality of the material remains a critical objective.

Achieving a high deposition rate can be facilitated through various approaches, including:

a) **Plasma Containment and Ion Density Optimization:** Employing earth shields to confine the plasma within the inter-electrode region, thereby preventing the diffusion of reactive species. Additionally, carefully increasing the power input to the plasma enhances the density of ionized species while mitigating undesired gas-phase polymerization reactions.
b) **Increase in Plasma Excitation Frequency:** Operating at higher excitation frequencies can contribute to improved deposition kinetics and (a-Si:H) thin films properties.
c) **Utilization of Higher Silane Radicals:** The incorporation of higher-order silane radicals can enhance the deposition efficiency. For the deposition of high-quality (a-Si:H) thin films, a lower power density, typically below 20 mW/cm², is conventionally employed. However, in this study, we focus on investigating the characteristics of (a-Si:H) thin films deposited at high power densities to evaluate their structural, electronic, and optoelectronic properties.

2. Experimental Details

This study presents a detailed investigation of RF plasma (13.56 MHz)-assisted deposition of hydrogenated amorphous silicon (a-Si:H) films, utilizing silane (SiH_4) as the precursor gas. The plasma was excited using a 13.56 MHz RF source (Model RF 5S), and substrates were positioned on the anode of the research reactor. The partial pressure of SiH_4 was precisely controlled using a Mass Flow Controller (MFC). To optimize the deposition rate (r_d), the RF power applied to the cathode was systematically varied across distinctive pressure conditions. The deposition parameters were as follows:

1) **Chamber Pressure:** 0.1–1.0 Torr
2) **Substrate Temperature:** 300°C
3) **SiH_4 Flow Rate:** 40.0 sccm
4) **Power Density:** Varied from 16 to 180 mW/cm²

The (a-Si:H) thin films thickness, measured using a Talystep profiler (Rank-Taylor Hobson), was approximately 1.5 µm. Comprehensive optical, electrical, and structural characterizations were performed following standard measurement protocols. For identification, the samples deposited at 1W and 21W RF power were designated as Sample no-HR-031 at 1 W and Sample no HR-022 at 7 W, respectively.

3. Results and Discussion

Deposition Rate

The deposition rate of the (a-Si:H) thin films was determined by dividing the measured film thickness by the deposition time. Film thickness was estimated using a Talystep (Rank-Taylor Hobson). The dependency of the deposition rate (r_d) on the applied RF power is illustrated in Figure 1.1. The results indicate a monotonic increase in (r_d) with increasing power. For the deposition of device-quality (a-Si:H) thin films, a low power density (<20 mW/cm²) is typically preferred. In this study, the deposition rate increased from 2.9 Å/s to 13 Å/s as the applied power was raised from 1 W to 21 W. The increase in RF power enhances the dissociation and ionization of silane molecules, leading to a higher flux of deposition precursors reaching the substrate surface, thereby promoting films growth.

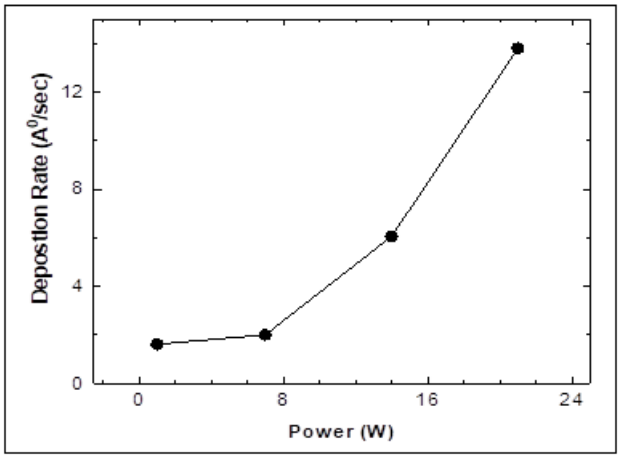

Figure 1.1: Illustrates the dependence of the deposition rate on the applied RF power

4. Optical Property

The investigation of the optical properties of semiconductors serves as a fundamental method for analyzing their electronic band structure, the frequencies of optical phonon modes, and other intrinsic material characteristics. In this study, the optical properties of the films were examined through absorption and transmission spectroscopy, performed at room temperature using a UV-Vis spectrophotometer (Ocean Optics).

4.1. Energy band gap

The absorption spectra of (a-Si:H) thin films were analyzed to determine the optical energy band gap within the spectral range of 400–1100 nm. A sharp increase in the absorption coefficient was observed below a specific wavelength, indicating strong optical absorption.

The energy band gap (Eg) was determined using the Tauc relation [5,6,7]:

$\alpha h\nu = A(h\nu - Eg)^n$

where:

- hν is the photon energy,
- α is the absorption coefficient,
- Eg is the optical band gap, and
- n=1/2 for direct band gap transitions.

To extract Eg, Tauc plot of $(\alpha h\nu)^{1/2}$ versus hν was constructed. The energy band gap was determined by extrapolating the linear portion of the plot to the $(\alpha h\nu)^{1/2}=0$ axis. Figure 1.2 presents the Tauc plot for plasma-deposited (a-Si:H) thin films, revealing a linear trend over a broad photon energy range, which confirms the presence of direct electronic transitions. From this analysis, the estimated energy band gap of (a-Si:H) thin films was found to be approximately 1.6 eV [8].

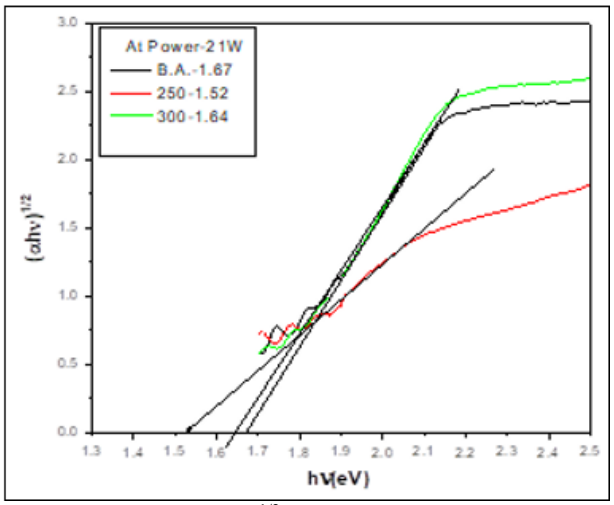

Figure 1.2: Plot of $(\alpha h\nu)^{1/2}$ on photon energy hν for a-Si:H thin films

4.2 Optical Constants

The optical constants, particularly the refractive index (nnn), of a thin film material can be determined from its transmission spectra. The transmission spectra of a-Si:H thin film samples within the spectral range of 400–1100 nm were analyzed to extract the optical parameters, as illustrated in the figures below. The transmittance interference pattern was enveloped to facilitate the determination of the refractive index, which was calculated using Manifacier's envelope method [4]

$$n = [N + (N^2 + n_0^2 n_1^2)^{1/2}]^{1/2}$$

where n_0 and n_1 represent the refractive indices of air and the substrate (glass), respectively. The parameter N is given by:

$$N = [(n_0^2+n_1^2)/2] + 2n_0n_1\,[T_{max} - T_{min}]/(T_{max}\times T_{min})]$$

T_{max} and T_{min} are the upper extreme point and lower extreme point of the envelope at a particular wavelength.

The extinction coefficient (k) is give by:

$$K = (-\lambda/4\,\pi t)\ln p$$

t is the thickness of the film.

$$P = C_1/C_2\,[1-T_{max}/T_{min}]/[1+T_{max}/T_{min}]$$

$$C_1 = (n+n_0)\,(n+n_2)$$

$$C_2 = (n-n_0)\,(n_1-n)$$

The thickness of these films was measured by a Spectrophotometer method using transmission spectra, which are given as:

$$t = M\,\lambda_1\,\lambda_2/2[n(\lambda_1)\,\lambda_2 - n(\lambda_2)\,\lambda_1]$$

M is the number of oscillation between the two extreme in the interference pattern of transmission spectra. λ_1 λ_2 and

$n(\lambda_1)$ $n(\lambda_2)$ are the corresponding wave lengths and indices of refraction.

At 1W**. Figure 1.3** illustrates the optical transmission spectra of sample number-031 at 1W, both as-deposited and post-annealing under vacuum conditions at 250°C and 300°C for one hour. The refractive index and extinction coefficient were calculated using Manifacier's method [4] and are summarized in **Table 1.1** for samples deposited on Corning 7059 glass substrates at 300°C. At an RF power of 1W and a gas flow rate of 0.5 Torr, the transmittance in the visible spectrum was initially ~30% before annealing. However, upon annealing at 250°C and 300°C, the transmittance increased significantly to ~80% and ~90%, respectively. This enhancement in optical transmittance is attributed to the diffusion of hydrogen atoms toward the film surface at elevated temperatures, facilitating the transition from an amorphous to a more crystalline phase.

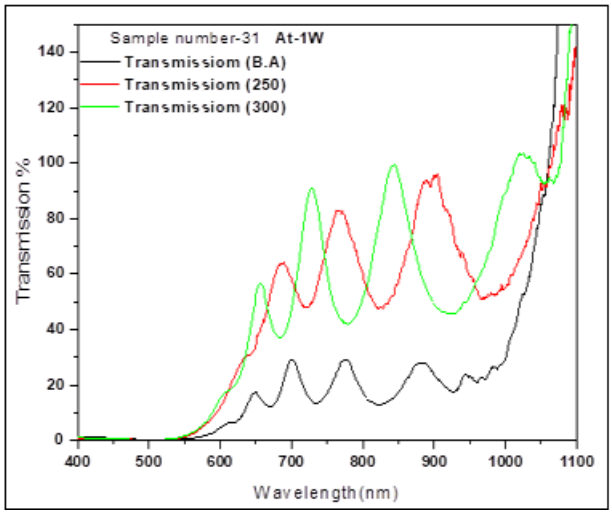

Figure 1.3: Typical transmission spectra of a-Si:H thin films, deposited on Corning 7059 glass substrates using the RF Plasma-Enhanced Chemical Vapor Deposition (RF-PECVD) technique, were examined before and after thermal annealing at 250°C and 300°C.

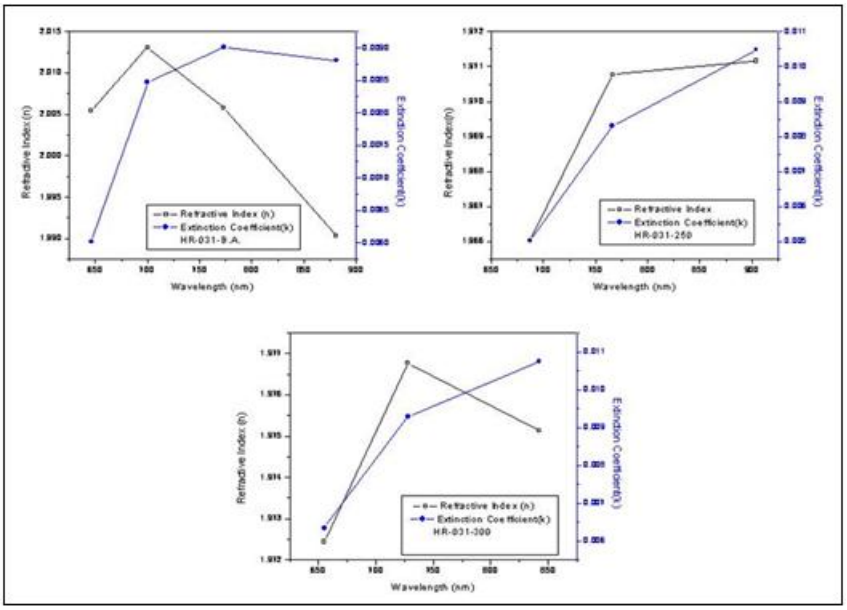

Figure 1.4: The refractive index and extinction coefficient as a function of wavelength for as- transferred and thermally annealed (a-Si:H) thin films samples

Figure 1.4 Show the variation of the refractive index and extinction coefficient as a function of wavelength for (a-Si:H) thin films deposited at RF power of 1W. The observed trends indicate that the refractive index and extinction coefficient exhibit distinct behaviors, which are influenced by the interaction between the incident wavelength and the material. The calculated values of the refractive index and extinction coefficient for different incident wavelengths are systematically presented in Table 1.1.

RF Power:	Wavelength	T_{MAX}	T_{MIN}	N	n	K
AT 1-W (Before annealing)	646	16.93	10.59	1.731086	2.005404	0.00602
	700	29	13.21	1.748652	2.013086	0.00847
	773	29	14.25	1.732078	2.005838	0.00901
	881	27.68	16.65	1.696799	1.990366	0.00881
At 1-W (Annealed at 250 oC)	687	63.79	47.18	1.641557	1.966018	0.00503
	766	82.74	47.18	1.652328	1.970777	0.00831
	904	95.63	50.35	1.653212	1.971167	0.01048
At 1-W (Annealed at 300 OC)	655	56.35	35.57	1.656102	1.972443	0.00635
	728	90.82	40.56	1.665932	1.976779	0.00929
	842	99.3	44.51	1.662189	1.975129	0.01074

Table (1.1): Calculation of the refractive index (n) and extinction coefficient (k) for (a-Si:H) thin films was performed for both as-deposited samples and those annealed at 250°C and 300°C. The values of n and k were determined using transmission spectra and Macinfacier's envelope method. The variations in these optical constants with respect to annealing temperature provide insights into structural modifications and phase transitions occurring within the material. **At Power 21W**

Figure (1.5) presents the optical transmission spectra of sample number HR-022 at 7 W, deposited on a Corning 7059 glass substrate at a temperature of 300°C using an RF power of 21W, with a maintained gas flow rate of 0.5 Torr. Prior to annealing, the refractive index (n) and extinction coefficient (k) were determined and are listed in Table (1.2). The films exhibit an average transmittance of approximately 60% in the visible spectrum. which remains largely unaffected even after annealing at 250 °C and 300 °C, indicating that annealing has slit influence on the transmittance properties of the (a-Si:H) thin films [9,10]., Figure (1.6) illustrates the variation of the refractive index and extinction coefficient as a function of wavelength of (a-Si:H) thin films deposited at an RF power of 7W. The observed trends in n and k are dependent on the interaction between the incident wavelength and the material properties of the (a-Si:H) thin films. The tabulated values of n and k for different incident wavelengths are provided in Table (1.2).

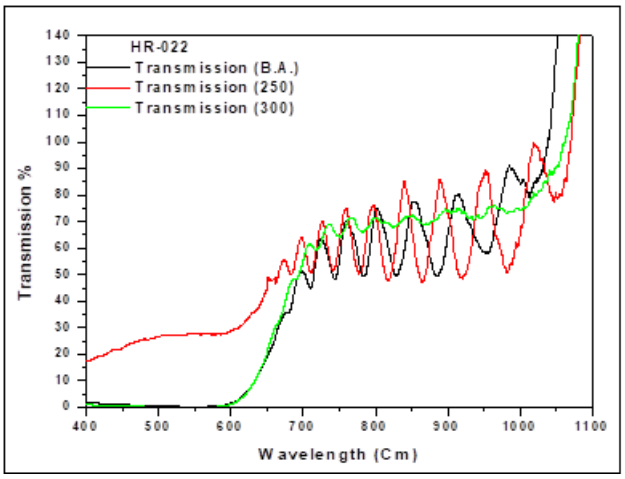

Figure 1.5: Typical optical transmission spectra of (a-Si:H) thin films, deposited on Corning 7059 glass substrates using the RF Plasma-Enhanced Chemical Vapor Deposition (RF-PECVD) technique, were observed before annealing and after annealing at 250°C and 300°C.

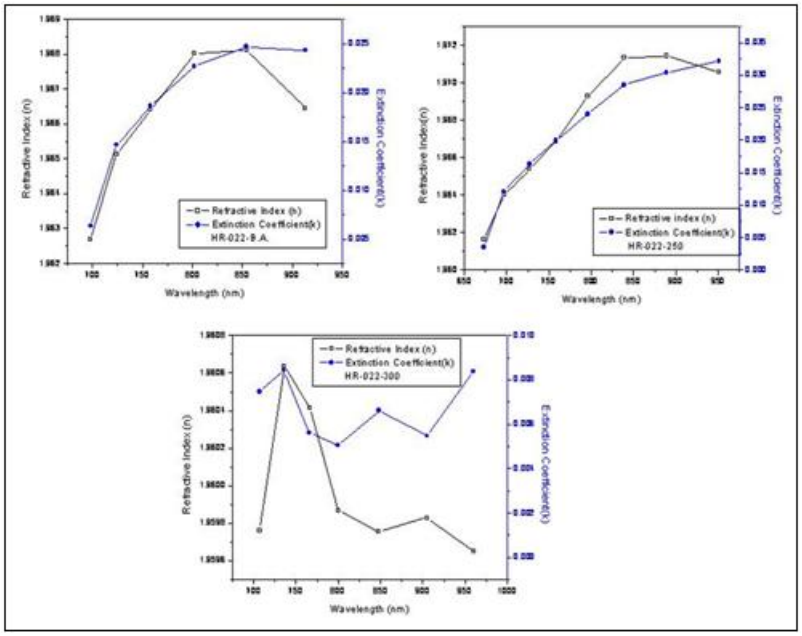

Figure 1.6: The variation of the refractive index (n) and extinction coefficient (k) as a function of wavelength for both as-deposited and annealed a-Si:H thin film samples was analyzed.

Table 1.2: Calculation of the refractive index (n) and extinction coefficient (k) for (a-Si:H) thin films before annealing and after annealing at 250°C and 300°C

RF Power	Wavelength (nm)	T_{MAX}	T_{MIN}	N	n	K
21W (Before Annealing)	726.46	62.99	49.5	1.799596	2.035279	0.011
	761.46	69.72	49.79	1.815798	2.04231	0.016
	804.21	74.23	50.52	1.754268	1.873109	0.025
Sample number-022, 250 °C	697.71	63.42	50.98	1.636543	1.963801	0.01041
	726.79	70.11	51.63	1.640316	1.965469	0.01511
	759.15	74.11	50.98	1.64341	1.966837	0.01981
	795.09	75.77	48.38	1.647416	1.968607	0.0244
	840.19	84.41	47.45	1.652684	1.970934	0.03203
	889.54	85.33	49.03	1.651029	1.970203	0.03369
	953.26	89.23	51.25	1.649916	1.969712	0.211607

	1019.6	99.45	78.37	1.633114	1.807271	
Sample number-022, 300 °C	69.01	735.86	717.4	1.625105	1.958739	0.005752
	71.19	766.9	750.73	1.625084	1.95873	0.003224
	71.49	799.25	781.93	1.625083	1.958729	0.16826
	72.41	847.6	824.57	1.625099	1.80283	

Table 1.3: Comparison of the transmittance values of (a-Si:H) thin films samples deposited at varying RF powers

Annealing Temperature	Transmittance (%) Sample Number-031 (Deposited at (1W)	Transmittance (%) Sample Number -022 Deposited at (21W)
Before Annealing	30	60
Annealing at 250 °C	50	61
Annealing at 300 °C	90	65

With an increase in RF power, the transmittance values exhibit a decreasing trend at higher wavelengths while increasing at lower wavelengths. At an applied power of 21W, the transmittance stabilizes and attains a constant value. Conclusion, this behavior remains unaffected by annealing temperature.

4.3. IR- Study

The infrared (IR) spectra of sample number-020, comprising a-Si:H thin films transferred on a (111) Si substrate at an applied RF power of 14W, were recorded in the spectral range of 500–2400 cm^{-1} before and after annealing at 250°C, as shown in Fig. (1.7).

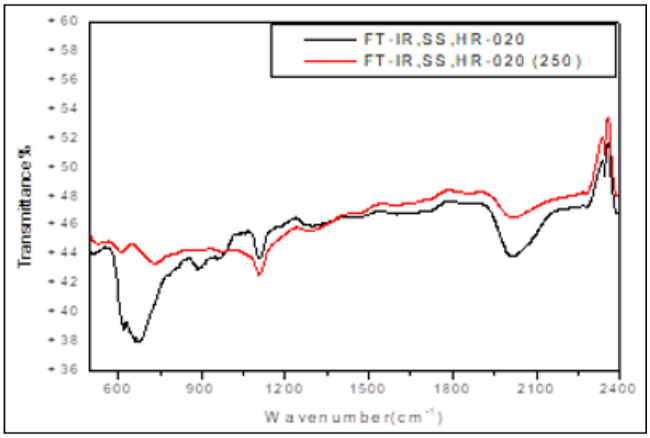

Figure 1.7: Representative IR transmission spectrum of a-Si:H thin films, deposited on a (111) Si substrate at an applied RF power of 14W, using the PECVD technique on Corning 7059 glass.

Several characteristic absorption features were recognized through analysis of the IR spectra. [11,12] A broad peak observed around 621 cm^{-1} and 606 cm^{-1} corresponds to the Si-H rocking/wagging mode before and after annealing, respectively. Additionally, bands at 630 cm^{-1} (rocking mode) and 862 cm^{-1} (symmetric deformation mode) are attributed to SiH_2 bonding, appearing both before and after annealing. It is evident from all analyzed samples that the shape and intensity of the IR spectra are significantly influenced by the deposition conditions.

A broad absorption feature around 2009 cm^{-1} (before annealing) and 2035 cm^{-1} (after annealing at 250°C) corresponds to Si-H stretching vibrations. These bands arise from SiH, SiH_2, and SiH_3 stretching modes. The substantial broadening of all absorption bands suggests the amorphous nature of the films, characterized by a wide distribution of bond angles for each vibrational mode and strong Columbic interactions among various local structural units.

We have plotted the PL spectrum recorded as deposited and annealed films at 350 nm wavelength of laser source for the sample deposited with R.F. power of 14W in Fig (3.13). At room temperature, the as deposited film PL spectrum show sharp Peaks at 2.07 eV, however the films annealed at higher temperature at 250 °C, PL peak position remains unchanged while change in PL intensity observed. For the films annealed at 300 °C we haven't found any change in PL peak positions and intensity when compared to that of the as deposited films. So we can say that the PL intensity first increases when annealing was done at 250 °C but on further increasing the annealing temperature to 300 °C the PL intensity decreases and reaches almost equal to that of the as deposited film.

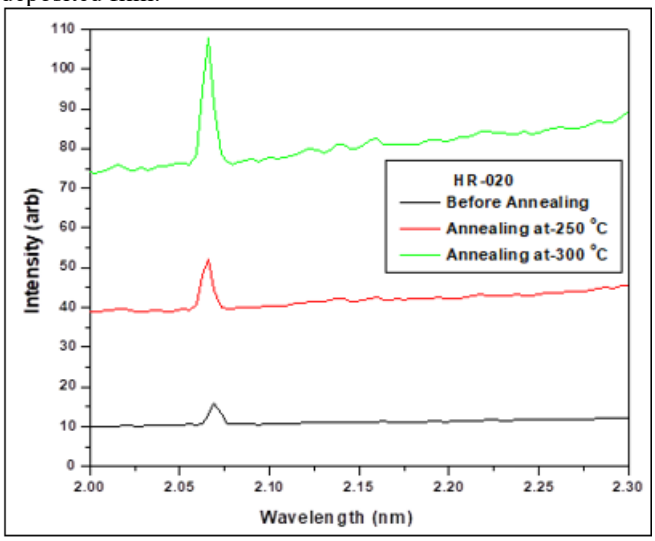

Figure 3.13: The PL spectra as function of photon energy for the a-Si:H films. As deposited and annealed samples. Annealing at 250 & 300 °C, this is deposited on (7059) corning glass substrate, by Radio Frequency PECVD Technique.

4.4 Laser Raman Raman spectroscopy

Raman scattering measurements have been widely recognized as a powerful technique for investigating the structural properties of hydrogenated amorphous silicon thin films (a-Si:H) and related materials (8-11). The first-order Raman spectrum of a-Si exhibits features associated with the crystalline phase, which are broadened due to structural disorder (12).

For the as-deposited a-Si:H thin film, synthesized via plasma deposition at an RF power of 14W and a substrate temperature of 300°C, the most intense transverse-optical

(TO) phonon mode shifts from approximately 460 cm^{-1} to 480 cm^{-1} (13). Upon annealing at 250°C and 300°C, this TO mode further shifts to approximately 470 cm^{-1} and 512 cm^{-1}, respectively [13,14]. The observed shift toward higher frequencies and the narrowing of the TO band are consistent with an improvement in short-range order, indicating a transition toward a more crystalline structure. In fully crystalline silicon, the TO mode exhibits a bandwidth of approximately 30 cm^{-1} at 512 cm^{-1}. The Raman spectroscopic setup used in this study encompasses of a Perkin Elmer-2000 FT-Raman system, incorporating a double monochromatic, photon-counting electronics, and an argon laser operating at a wavelength of $\lambda = 514.5$ nm, with an incident power of approximately 120 mW cm^{-2} directed onto the film plane. All measurements were performed at room temperature in ambient conditions.

Figure (1.8) presents a typical Raman spectrum of a-Si:H. thin films. The full width at half maximum (FWHM) of the TO-like phonon band ΔwTO was used as a parameter to quantify the structural disorder in the Si-Si bonding network of a-Si:H (14,9). The TO-like phonon band, exhibiting a peak at 475–480 cm^{-1}, It exhibits asymmetric, likely attributable to the presence of the longitudinal-optical (LO)-like band at 410 cm^{-1} (9). The broadening of the TO mode is characterized by the parameter ΔwTO, defined as $\Delta wTO = 2\Gamma(H)$ (15), where Γ(H) represents the half-width at half-maximum (HWHM) attained from the higher-frequency side of the TO-like band.

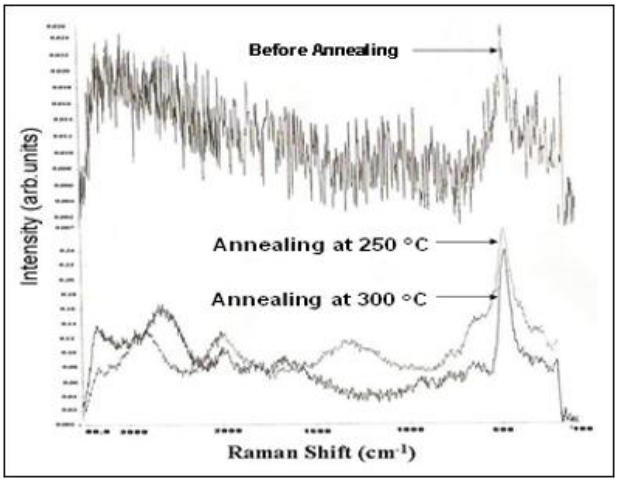

Figure 3.12: Typical Raman spectra of a-Si:H thin films before annealing and after annealing at 250°C and 300°C.

Conductivity and photoconductivity

Variation of dark and photo-conductivity with temperature of a-Si:H deposited at 1W, as deposited and annealed at 250 & 300 °C temperature. It is clear from the figure that after annealing, the dark and photoconductivity values are increase as compared to as deposited film. This may be because of surface passivation [15]. In addition, the photo response is increase after annealing which may be due to the reduction of structural defects in the network. At this annealing temperature a-Si:H film shows the transport properties of as deposited μc-Si:H films. This might be due to the phase transition of these films from amorphous to microcrystalline at this annealing temperature. As we start annealing, hydrogen content in the structure decreases because of the dissociation of hydrogen bonds. Thus, most of the SiH_3 bonds disappeared, which may be related with the increment of crystallinity. This is in agreement with the data of room temperature conductivity, which show that σ_d increases with annealing temperature. Has only increased the deposition rate, which is obvious but has no effect on the photo and dark conductivities. The values of the photo and dark conductivities are tabulated in Table (1.4).

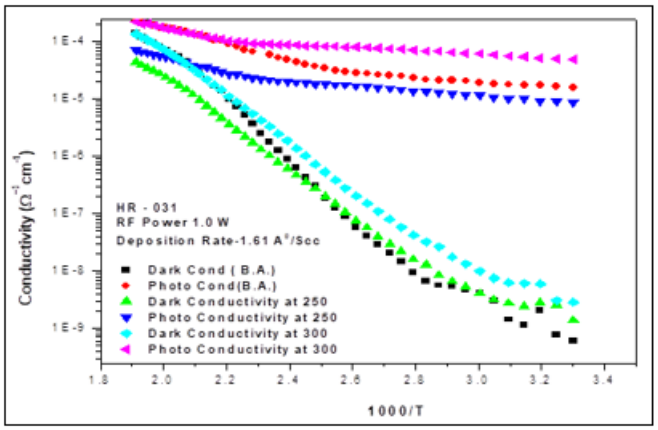

Figure 1.4: Variation of dark conductivity and photoconductivity as a function of 100/T K for HR-031, a-Si:H thin film deposited on (7059) corning glass substrate at a power of 1W.

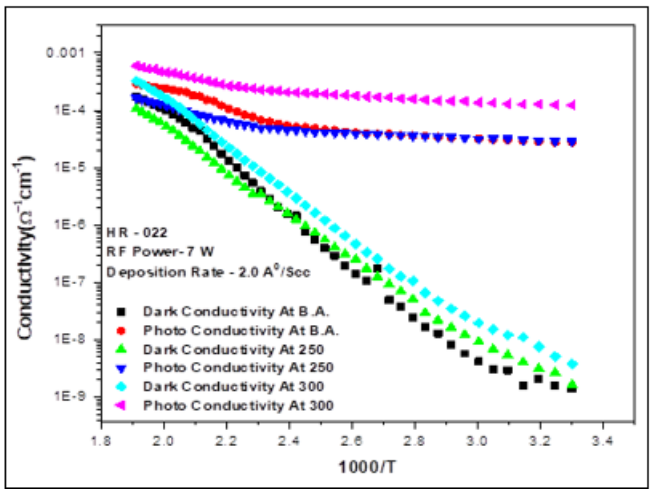

Figure 1.5: Variation of dark conductivity and photoconductivity as a function of 100/T K for HR-019, a-Si:H deposited on (7059) corning glass substrate at a power of 7W.

Table (1.4): Variation of Conductivity σ_d and photoconductivity σ_{ph} of a-Si:H thin films, as deposited and annealing at 250, 300 °C.

S. No.	Power (W)	Before Annealing (30 oC)		After Annealing (250 oC)		After Annealing (300 oC)	
		$\sigma d(\Omega^{-1}cm^{-1})$	$\sigma ph(\Omega^{-1}cm^{-1})$	$\sigma d(\Omega^{-1}cm^{-1})$	$\sigma ph(\Omega^{-1}cm^{-1})$	$\sigma d(\Omega^{-1}cm^{-1})$	$\sigma ph(\Omega^{-1}cm^{-1})$
HR-031	1.0 W	$5.94X10^{10}$	$1.58X10^{-5}$	$1.40X10^{-9}$	$8.67X10^{-6}$	$2.8X10^{-9}$	$4.9X10^{-5}$
HR-022	7 W	$1.52X10^{-8}$	$4.40X10^{-3}$	$4.25X10^{-8}$	$1.59X10^{-3}$	$2.0X10^{-6}$	$2.6X10^{-5}$

XRD

We have characterized the samples by X-ray diffractometer using copper tube at a wavelength of 1.54 A. The XRD scan of the sample deposited at 1W power is show in the Fig (1.6). It is observe that the as deposited sample is amorphous in nature. When the sample is annealed at 250 ^{o}C for one hour in vacuum then some peaks namely (220) and (332) begin to appear which shows that the sample is becoming crystalline. When we have annealed the sample at higher temperature of 300 ^{o}C then some more peaks along with these appeared in the sample annealed at 250 ^{o}C began to appear and are shown in Fig (1.6). However, it is also observed that the sample even after annealing at 300 ^{o}C has not become crystalline, as the peaks are not so dominant that we cannot calculate the particle size using scherrer's formula.

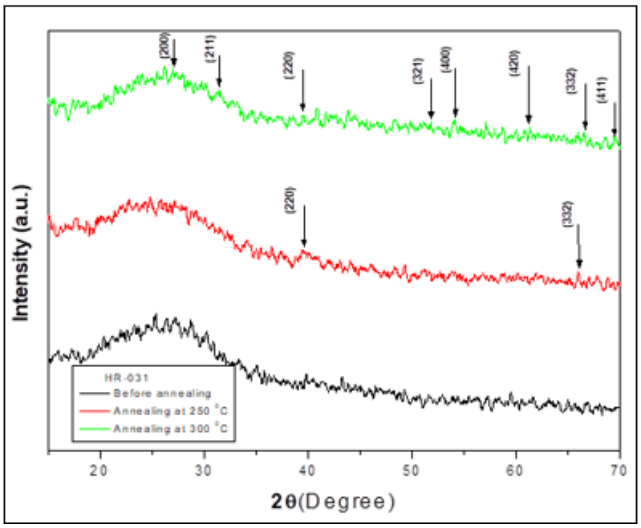

Figure 1.6: The glance incidence angle XRD spectra of HR-031 a-Si:H thin films deposited at 7059 glass substrate, and annealing at various temperatures

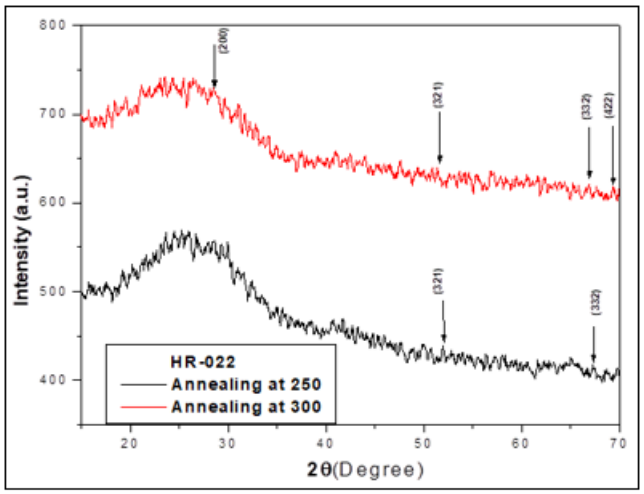

Figure 1.7: The glance incidence angle XRD spectra of HR-022 a-Si:H thin films deposited at 7059 glass substrate, and annealed at various temperature

AFM

Typical surface morphology of a-Si:H film deposited by PECVD at a Power of 7W are presented in the AFM Micrograph. These sample (at 7W) have been annealed in vacuum for one hour at 250 ^{0}C and 300 ^{0}C. The 0.5µm x 0.5µm AFM micrographs of the annealed films are shown in **Fig 1.8 (a,b, c & d)** respectively**.** An increase in the particle size with increase in the annealing temperature. We have calculated particle size from the AFM micrographs and are tabulated in Table (1.5). The 3D AFM images of the annealed films are shown in Fig (1.5) (a,b ,c& d). From these images, we have calculated the effect of the annealing on the roughness of the samples. It has been observe, that with increase in the annealing temperature the roughness increases. We know that increase in roughness results in decrease in transmittance. The same have been observe in the Transmission graphs which shows decrease in transmittance with increase in annealing temperature. The rms values of the roughness are tabulated in Table (1.5).

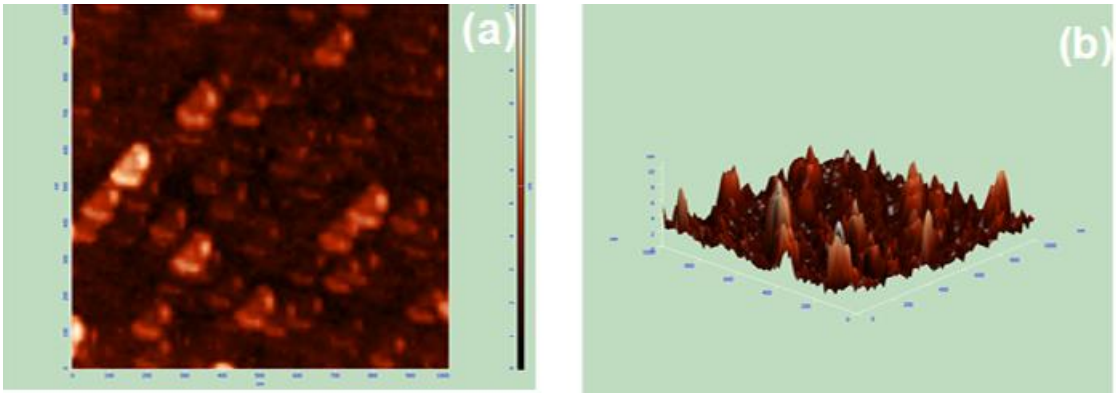

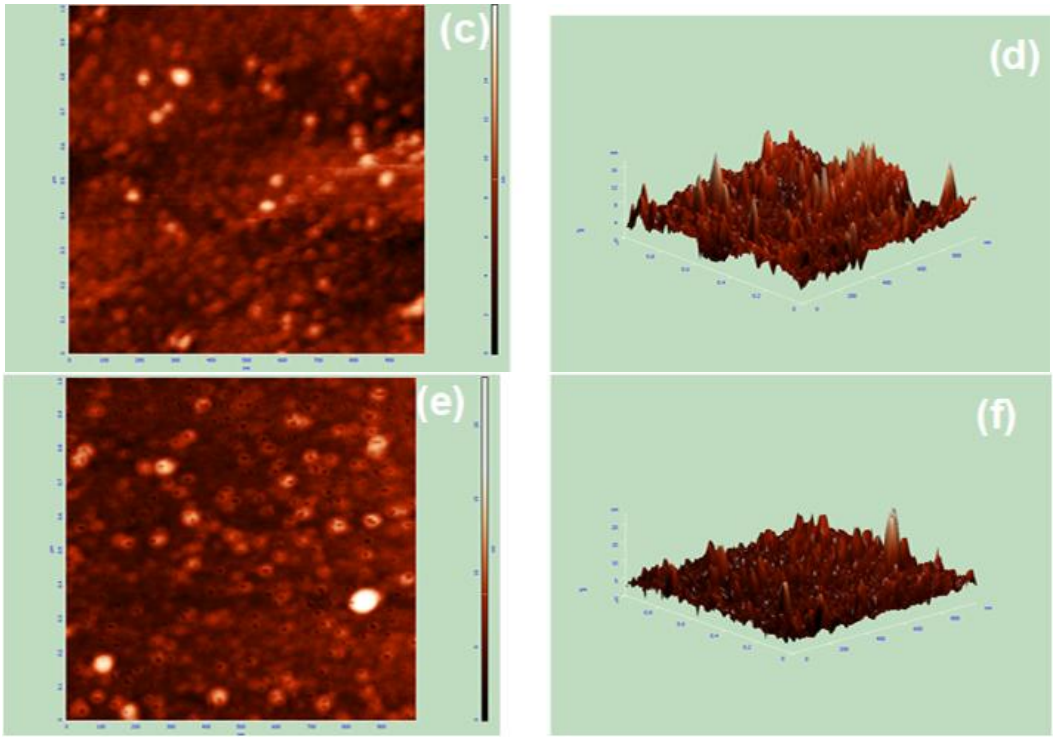

Figure 1.8: The AFM micrograph of Sample Number HR-031

Table (1.5): Measured properties using AFM of sample HR -022 (deposited at a power of 21W)

Sample No	Annealing Temperature (0C)	Partical Size dAFM (nm)	rms Roughness (nm)
At 7W	As Deposited	16	3.89883
	250	23	3.4948
	300	29	3.0945

SEM

We have analyzed the sample deposited at a power of 7 W using Fe-SEM. The images of the samples are show in figure. It is clearly show Fig 1.9 (a) that the sample before annealing was smooth but there is no indication of grains in it. But as the sample is annealed at 250 ^{0}C the grain growth takes place which is evident from the figure Fig 1.9 (b). As the annealing temperature is raised up to 300 ^{0}C the size of the grains increases and it is shown in Fig 1.9 (c). With increase in annealing temperature the rearrangement of the atoms takes place and these results in grain growth.

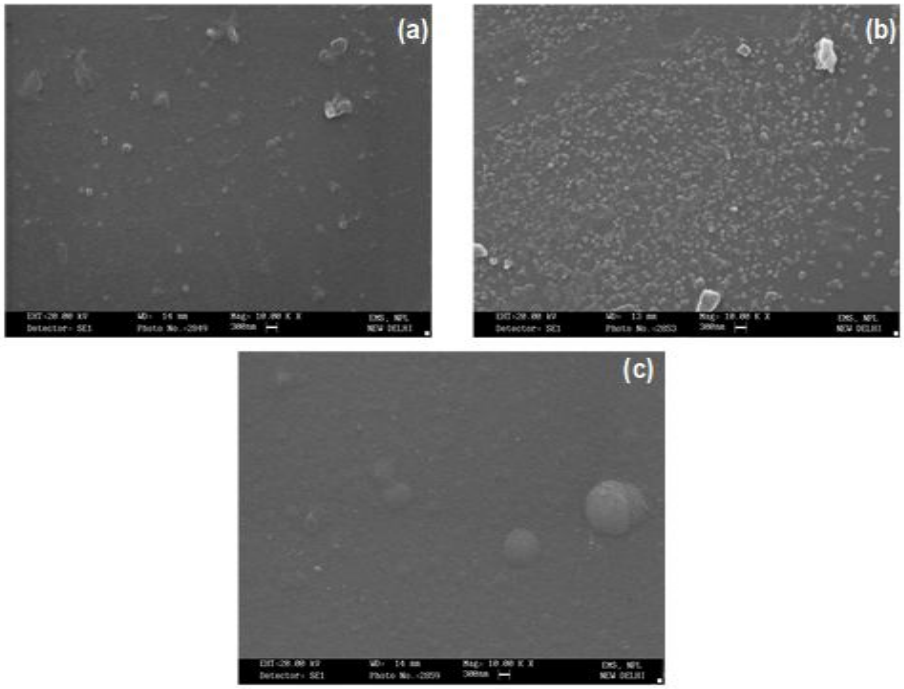

Figure 1.9 (a, b, c): Typical SEM micrograph of sample no Sample Number HR-022 of a-Si:H films deposited at a power of 7W before annealing and after annealing at 250 ^{0}C & 300 ^{0}C respectively.

5. Conclusions

a-Si:H layers, synthesized via PECVD, have garnered significant interest due to their promising applications in electronic and photovoltaic devices. Conventionally, the crystallization of a-Si:H films is induced through external techniques such as laser irradiation or the incorporation of metal catalysts. However, our investigation reveals that films deposited via the PECVD process inherently exhibit nanocrystal line regions embedded within the amorphous silicon matrix, eliminating the necessity for external crystallization stimuli.

Moreover, Thermal annealing under vacuum conditions at comparatively low temperatures of 250°C and 300°C promotes the substantial growth of these embedded crystallites, leading to an enhanced crystalline fraction and improved spatial distribution. This thermally induced crystallization is expected to refine the structural and optical characteristics of the material, rendering it more viable for advanced technological applications. To comprehensively analyse the structural transformations in these films, we utilized multiple characterization techniques, [15,16,17] including UV-VIS spectrophotometry for optical absorption analysis, Raman spectroscopy for assessing structural order and crystallite size, and Fourier-transform infrared (FT-IR) spectroscopy for examining the chemical bonding states within the material.

Acknowledgement
The authors express their gratitude to the University Grants Commission (UGC), Government of India, for financial support. Additionally, we acknowledge the National Physical Laboratory (NPL), New Delhi, for providing access to experimental facilities.

References

[1] R.A. Street, Hydrogenated amorphous silicon, Cambridge University Press (1991).
[2] T. Gruszecki and B. Holmstrom, Solar Energy Materials and solar cells, 31(1993) 227.
[3] J.C. Manifacier, J. Gasiot, J.P. Fillard, J. Phys. E, 9(1976)1002.
[4] M.Hirose, in semiconductor and semimetals 21, A ed.j.i. Pankove (academic Press, New Yark (1984). P. 9.
[5] Tauc J, Ed, Amorphous and Liquid Semiconductor (Plenum Press New York) (1974) 159.
[6] T. Moss, Optical Properties of semiconductors (Butter Worths), London.
[7] O, S. T. Ishidate, K . Inoue, K . Tsuji and S. Minomusa, Solid state Commun. 24. 197 (1982).
[8] J. S. Lannin, L. J. Pilione, S. T. Kashiragar, R. Messier and R.C. Ross, Phys. Rev. Lett. 26, 3506 (1982). (1). Tsu, J. Gonzalez- Hernandez, J. Doehler and S.R. Ovshinsky, Solid State Commun. 46, 79 (1983).
[9] A. Morimoto, S. Oozora, M. Kumeda and T. Shimizu, Solid State Commun, 47,773 (1983).
[10] J. S. Lannin, in Semiconductor and Semimetals 21 B. ed. J. I. Pankove (Academic New York, 1984), p. 159.
[11] Y. Hishikawa, K. Watanabe, S. Tsuda, M. Ohnishi and Y. Kuwano, Jpn. J. Appl. Phys. 24, 385 (1985).
[12] T. Ishidate, K. Inoue, K. Tsuji and S. Minomusa, Solid state Commun. 24. 197 (1982).
[13] I. Sakata, M. Yamanaka. S. Okazaki and Y. Hayashi, Appl. Phys. A 48, 295 (1989).
[14] Heavens optical properties of thin solid films, dover New York (1965).
[15] J.A. Reimer and J. C. Knights: In Tetrahedrally Bonded Amorphous Semiconductors, edit. R. A. Street, D. K. Siegelsen, and J. C. knights (American Institute of Physics, new York, 1981, p. 78.).
[16] **Structural investigation of hydrogenated amorphous silicon by X-ray diffraction**
[17] W. Schülke,Pages 451-468 | Received 22 Mar 1980, Accepted 10 Jun 1980, Published online: 20 Aug 2006. **Progress in solar cells from hydrogenated amorphous silicon,** Michael Stuckelberger [a b], Rémi Biron [a], Nicolas Wyrsch [a], Franz, Josef Haug [a], Christophe Ballif [a] , **Renewable and Sustainable Energy Reviews**,Volume 76, September 2017, Pages 1497-1523
[18] Mechanism of hydrogen-induced crystallization of amorphous silicon, Saravanapriyan Sriraman, Sumit, Agarwal, Eray S. Aydil & DimitriosMaroudas ,*Nature* **volume 418**, page s62–65 (2002), 04 July 2002.